Scaling Law of Seismic Spectrum

KEIITI AKI

Department of Geology and Geophysics
Massachusetts Institute of Technology, Cambridge

The dependence of the amplitude spectrum of seismic waves on source size is investigated on the basis of two dislocation models of an earthquake source. One of the models (by N. Haskell) is called the ω^3 model, and the other, called the ω^2 model, is constructed by fitting an exponentially decaying function to the autocorrelation function of the dislocation velocity. The number of source parameters is reduced to one by the assumption of similarity. We found that the most convenient parameter for our purpose is the magnitude M_s, defined for surface waves with period of 20 sec. Spectral density curves are determined for given M_s. Comparison of the theoretical curves with observations is made in two different ways. The observed ratios of the spectra of seismic waves with the same propagation path but from earthquakes of different sizes are compared with the corresponding theoretical ratios, thereby eliminating the effect of propagation on the spectrum. The other method is to check the theory with the empirical relation between different magnitude scales defined for different waves at different periods. The ω^2 model gives a satisfactory agreement with such observations on the assumption of similarity, but the ω^3 model does not. We find, however, some indications of departure from similarity. The efficiency of seismic radiation seems to increase with decreasing magnitude if the Gutenberg-Richter magnitude-energy relation is valid. The assumption of similarity implies a constant stress drop independent of source size. A preliminary study of Love waves from the Parkfield earthquake of June 28, 1966, shows that the stress drop at the source of this earthquake is lower than the normal value (around 100 bars) by about 2 orders of magnitude.

INTRODUCTION

Elaborate studies have been made in recent years to find seismic source parameters such as fault length, rupture velocity, and stress drop at the earthquake source from the spectrum of seismic waves. Except for the geometric parameters obtained from fault plane studies, however, the magnitude is the only physical parameter that specifies most earthquakes. A gap exists between the two approaches currently used, one based on the use of spectrum and the other on amplitude. The purpose of the present paper is to fill this gap by finding a first approximation to the relation between seismic spectrum and magnitude of earthquakes on the basis of some dislocation models of earthquake sources. For this purpose we must reduce to one the number of parameters specifying a dislocation. We shall make this reduction by assuming that large and small earthquakes satisfy a similarity condition.

The relation between seismic spectrum and earthquake magnitude is not a new problem. It has been well known that the greater the size of an earthquake, the more efficiently longer-period waves are generated. In the early days of seismology in Japan, much attention was given to the presence of large long-period motion in P waves from large local earthquakes [cf. *Matuzawa*, 1964]. Analyses of seismic waves by *Jones* [1938], *Honda and Ito* [1939], *Gutenberg and Richter* [1942], *Byerly* [1947], *Kanai et al.* [1953], *Asada* [1953], *Aki* [1956], *Kasahara* [1957], *Matumoto* [1960], and others have shown that the period of the spectral peak for P waves, S waves, surface waves, and even for coda waves increases with earthquake magnitude.

The most convincing evidence for the greater efficiency of generating long-period waves by larger earthquakes is probably given by *Berckhemer* [1962]. He compared seismograms obtained at a station from two earthquakes of the same epicenter but of different size. We shall reproduce his result later.

The magnitude of an earthquake is defined as a logarithm of amplitude of a certain kind of seismic wave recorded by a certain type of band-limited seismograph. If there is such a size effect on seismic spectra as mentioned

above, the unit of magnitude obtained from one kind of wave recorded by one type of seismograph may not correspond to that obtained from another kind of wave recorded on another instrument. In fact, *Gutenberg and Richter* [1956*a*] discovered a discrepancy between the magnitude scale based upon short-period body waves and that based upon long-period surface waves.

It will be shown that the theoretical scaling law of the seismic spectrum derived from a dislocation model of the earthquake source satisfactorily explains the above-mentioned observations.

Theoretical Models of the Earthquake Source

Following *Haskell* [1966], we define a dislocation function $D(\xi, t)$ which is the displacement discontinuity across a fault plane at a point ξ and time t. The fault plane extends along the ξ axis, and $D(\xi, t)$ is considered as the average dislocation over the width w of the fault. Taking the starting point of the fault at the origin of the (x, y, z) coordinates, and the ξ axis along the x axis, we assume that the fault ends at $\xi = L$ and the surrounding medium is infinite, isotropic, and homogeneous. Introducing polar coordinates (r, θ, φ) by the relation

$$\begin{aligned} x &= r\cos\theta \\ y &= r\sin\theta\cos\varphi \\ z &= r\sin\theta\sin\varphi \end{aligned} \tag{1}$$

the displacement components of P and S waves at long distances, corresponding to a source of longitudinal shear fault [*Haskell*, 1964] for example, can be written as

$$U_r = \frac{1}{4\pi br}\left(\frac{b}{a}\right)^3 \sin 2\theta \sin\varphi \cdot w\int_0^L \dot{D}\left(\xi, t - \frac{r - \xi\cos\theta}{a}\right) d\xi$$

$$U_\varphi = \frac{1}{4\pi br}\cos\theta\cos\varphi \cdot w\int_0^L \dot{D}\left(\xi, t - \frac{r - \xi\cos\theta}{b}\right) d\xi \tag{2}$$

$$U_\theta = \frac{1}{4\pi br}\cos 2\theta \sin\varphi \cdot w\int_0^L \dot{D}\left(\xi, t - \frac{r - \xi\cos\theta}{b}\right) d\xi$$

where a and b are the velocities of P and S waves, respectively. The above expressions have the following common form:

$$U = P(r, \theta, \varphi, a, b) \cdot w\int_0^L \dot{D}\left(\xi, t - \frac{r - \cos\theta}{c}\right) d\xi \tag{3}$$

where c is the appropriate wave velocity. In terms of the Fourier transform, the above form can be written as

$$U(\omega) = P(r, \theta, \varphi, a, b)\, A(\omega) \tag{4}$$

where

$$\begin{aligned} U(\omega) &= \int_{-\infty}^{\infty} u(t) e^{-i\omega t}\, dt \\ A(\omega) &= w\int_{-\infty}^{\infty} e^{-i\omega t}\, dt \cdot \int_0^L \dot{D}\left(\xi, t - \frac{r - \xi\cos\theta}{c}\right) d\xi \end{aligned} \tag{5}$$

If the medium is dissipative, the equation corresponding to (4) will be

$$U(\omega) = P[r, \theta, \varphi, a, b, \omega, Q(\omega)] \cdot A(\omega) \tag{6}$$

where $Q(\omega)$ is the dissipation coefficient. The above expression shows that we can isolate the propagation term $P(\omega)$ which does not, except for the direction of fault propagation, include the fault motion parameters. Mathematically, such a simple isolation is not permitted for an arbitrary heterogeneous medium. Practically, however, this separation of propagation factor from source factor may be permitted, at least as a good first approximation. In this paper we shall be concerned only with the source factor $A(\omega)$, which can be calculated from the dislocation $D(\xi, t)$ according to (5).

For comparison with observations we shall use seismic waves observed at a given station from distant earthquakes of the same epicenter, the same focal depth, and the same fault plane solution, but of different magnitude. The ratio of the Fourier transforms of two such seismograms may be directly compared with the

theoretical ratio for the source factor $A(\omega)$, because the propagation factor $P(\omega)$ may be canceled in the observed ratio. This ingenious method comes from *Berckhemer* [1962]. His theoretical model, however, seems unrealistic, because, from the point of dislocation theory, his model implies that the amount of dislocation is constant, independent of the size of the fault.

Following the general line of approach taken by *Haskell* [1966], we introduce the autocorrelation function $\psi(\eta, \tau)$ of $\dot{D}(\xi, t)$:

$$\psi(\eta, \tau) = \iint_{-\infty}^{\infty} \dot{D}(\xi, t)\dot{D}(\xi + \eta, t + \tau)\, d\xi\, dt \tag{7}$$

Putting the Fourier transform of $\psi(\eta, \tau)$ as $\hat{\psi}(k, \omega)$, we get

$$\hat{\psi}(k, \omega) = \iint_{-\infty}^{\infty} \psi(\eta, \tau)e^{-i\omega\tau+ik\eta}\, d\tau\, d\eta \tag{8}$$

$$\psi(\eta, \tau) = \frac{1}{4\pi^2} \iint_{-\infty}^{\infty} \hat{\psi}(k, \omega)e^{i\omega\tau-ik\eta}\, d\omega\, dk \tag{9}$$

On the other hand, $A(\omega)$ can be rewritten by changing the order of integration and putting $t' = t - (r - \xi \cos\theta)/c$ in (5) as follows:

$$A(\omega) = we^{-i\omega r/c} \iint_{-\infty}^{\infty} \dot{D}(\xi, t') \cdot e^{-i\omega t'+i\omega\xi\cos\theta/c}\, dt'\, d\xi \tag{10}$$

In the above expression the integration limits are extended to infinity by putting $\dot{D}(\xi, t) = 0$ for $\xi < 0$ and $L < \xi$. Putting the Fourier transform of $\dot{D}(\xi, t)$ as $B(k, \omega)$, we obtain

$$B(k, \omega) = \iint_{-\infty}^{\infty} \dot{D}(\xi, t)e^{-i\omega t+ik\xi}\, dt\, d\xi$$
$$\dot{D}(\xi, t) = \frac{1}{4\pi^2} \iint_{-\infty}^{\infty} B(k, \omega)e^{i\omega t-ik\xi}\, d\omega\, dk \tag{11}$$

Then we have from (10) and (11)

$$A(\omega) = we^{-i\omega r/c}B\left(\frac{\omega \cos\theta}{c}, \omega\right) \tag{12}$$

and

$$|A(\omega)|^2 = w^2 \left|B\left(\frac{\omega \cos\theta}{c}, \omega\right)\right|^2 \tag{13}$$

On the other hand, we get from (7) and (11)

$$\psi(\eta, \tau) = \frac{1}{4\pi^2} \iint_{-\infty}^{\infty} \dot{D}(\xi, t) \iint_{-\infty}^{\infty} B(k, \omega) \cdot e^{i\omega(t+\tau)-ik(\xi+\eta)}\, dk\, d\omega\, d\xi\, dt$$
$$= \frac{1}{4\pi^2} \iint_{-\infty}^{\infty} B(k, \omega)B(-k, -\omega) \cdot e^{i\omega\tau-ik\eta}\, dk\, d\omega$$
$$= \frac{1}{4\pi^2} \iint_{-\infty}^{\infty} |B(k, \omega)|^2 \cdot e^{i\omega\tau-ik\eta}\, dk\, d\omega$$

Comparing this formula with (9), we get the well-known relation

$$\hat{\psi}(k, \omega) = |B(k, \omega)|^2 \tag{14}$$

Finally, we get from (9), (13), and (14) the relation between the amplitude spectral density $|A(\omega)|$ and the Fourier transform of the autocorrelation function:

$$|A(\omega)|^2 = w^2\hat{\psi}[(\omega \cos\theta)/c, \omega] \tag{15}$$

Thus, the source factor $|A(\omega)|$ of the amplitude spectral density is expressed in terms of the autocorrelation of dislocation velocity $\dot{D}(\xi, t)$. We followed *Haskell* [1966] in deriving the expressions above. Haskell, however, calculated the energy spectral density from the autocorrelation function $\Phi(\eta, \tau)$ of dislocation acceleration $\ddot{D}(\xi, t)$:

$$\Phi(\eta, \tau) = \iint_{-\infty}^{\infty} \ddot{D}(\xi, t)\ddot{D}(\xi + \eta, t + \tau)\, d\xi\, dt \tag{16}$$

The Fourier transform $\hat{\Phi}(k, \omega)$ of this function is related to $\hat{\psi}(k, \omega)$ simply by

$$\hat{\Phi}(k, \omega) = \omega^2\hat{\psi}(k, \omega) \tag{17}$$

Thus, we obtain

$$|A(\omega)|^2 = \frac{w^2}{\omega^2}\hat{\Phi}[(\omega \cos\theta)/c, \omega] \tag{18}$$

As shown above, the amplitude spectral density of seismic waves can be expressed in terms of the autocorrelation function of $\dot{D}(\xi, t)$ or that of $\ddot{D}(\xi, t)$. The autocorrelation function of $\dot{D}(\xi, t)$ can be determined if the absolute value of the Fourier transform of $\dot{D}(\xi, t)$ is given. There are an infinite number of space-time functions that have a common spectral density

but have different phases. By specifying an autocorrelation, therefore, we are considering an infinite group of space-time functions. The model based upon the autocorrelation function is different from the deterministic one in this respect and may be called 'statistical,' as was done by *Haskell* [1966].

Since the earthquake is essentially a transient phenomenon, however, the autocorrelation function introduced here cannot be treated in the same manner as the one for the stationary time series. The following figures will schematically illustrate what form may be expected for the autocorrelation function for the dislocation process at an earthquake source. Let the dislocation start at $\xi = 0$ and propagate along the ξ axis with a constant velocity v; then the dislocation at ξ will be zero for $t < \xi/v$ and will take a constant value $D_0(\xi)$ for $t > T + \xi/v$. Figure 1 shows a schematic picture of $D(\xi, t)$ at a given ξ. The corresponding $\dot{D}(\xi, t)$ and $\ddot{D}(\xi, t)$ are also shown in Figure 1. Their autocorrelation functions are shown schematically in Figure 2. The dashed lines in these figures are for the case in which the dislocation takes the form of a ramp function in time. We now construct two earthquake source models by fitting simple formulas to the two autocorrelation functions.

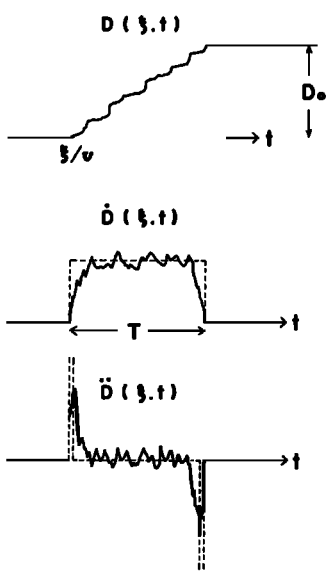

Fig. 1. Schematic diagram of dislocation and its time derivatives at a given point ξ on a fault.

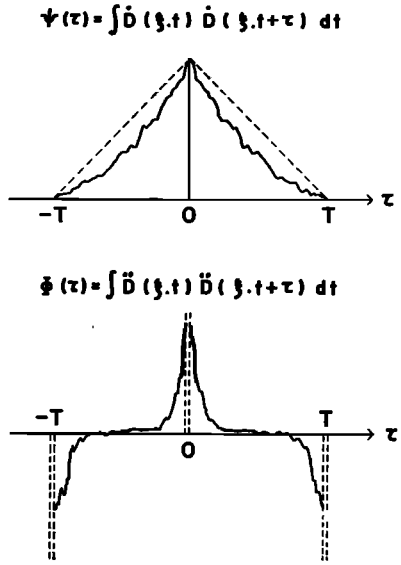

Fig. 2. Schematic diagram of autocorrelation functions of dislocation velocity and dislocation acceleration at a given point ξ on a fault.

In our first model, we assume that the temporal autocorrelation function of dislocation velocity decreases exponentially with the lag τ, that is

$$\int_{-\infty}^{\infty} \dot{D}(\xi, t)\dot{D}(\xi, t + \tau)\, dt = \psi_0 e^{-k_T|\tau|} \qquad (19)$$

Our second model is the one proposed by Haskell. He assumes that the autocorrelation function of dislocation acceleration takes the following form:

$$\int_{-\infty}^{\infty} \ddot{D}(\xi, t)\ddot{D}(\xi, t + \tau)\, dt = \Phi_0(1 - k_T|\tau|)e^{-k_T|\tau|} \qquad (20)$$

We shall assume an identical spatial correlation function for both models. The correlation between the dislocation velocity at ξ and t and that at $\xi + \eta$ and $t' = t + \eta/v$, that is

$$\int_{-\infty}^{\infty} \dot{D}(\xi, t)\dot{D}(\xi + \eta, t + \eta/v)\, d\xi$$

will indicate the degree of persistency of fault propagation. The persistency will decrease with the distance η between the two points. Following Haskell, we shall adopt the functional form of $e^{-k_L|\eta|}$ for this expression and also for the corresponding function of $\ddot{D}(\xi, t)$.

The above temporal and spatial autocorrelation functions are expressed in a single form, if we write

$$\psi(\eta, \tau) = \iint_{-\infty}^{\infty} \dot{D}(\xi, t)\dot{D}(\xi + \eta, t + \tau)\, d\xi\, dt = \psi_0 e^{-k_L|\eta| - k_T|\tau - \eta/v|} \quad (21)$$

for the first model, and

$$\Phi(\eta, \tau) = \iint_{-\infty}^{\infty} \ddot{D}(\xi, t)\ddot{D}(\xi + \eta, t + \tau)\, d\xi\, dt = \Phi_0 e^{-k_L|\eta|}\{1 - k_T|\tau - \eta/v|\} \cdot e^{-k_T|\tau - \eta/v|} \quad (22)$$

for the second model. Their Fourier transforms are

$$\hat{\psi}(k, \omega) = \frac{4k_T k_L \psi_0}{\{k_L^2 + (k - \omega/v)^2\}(k_T^2 + \omega^2)} \quad (23)$$

$$\hat{\Phi}(k, \omega) = \frac{8k_T k_L \Phi_0 \omega^2}{\{k_L^2 + (k - \omega/v)^2\}(k_T^2 + \omega^2)^2} \quad (24)$$

Using (15) and (23), we may obtain the source factor of amplitude spectral density for our first model as follows:

$$|A(\omega)| = \frac{w\sqrt{4k_T k_L \psi_0}}{\left[k_L^2 + \left(\frac{\cos\theta}{c} - \frac{1}{v}\right)^2 \omega^2\right]^{1/2} (k_T^2 + \omega^2)^{1/2}} \quad (25)$$

To determine the value of ψ_0, we put $\omega = 0$ in (10). Then

$$|A(0)| = w \iint_{-\infty}^{\infty} \dot{D}(\xi, t)\, dt\, d\xi = w \int_{-\infty}^{\infty} D_0(\xi)\, d\xi \quad (26)$$

Comparing the above equation with (25), we get

$$\frac{\sqrt{4k_T k_L \psi_0}}{k_T k_L} = w \int_{-\infty}^{\infty} D_0(\xi)\, d\xi \quad (27)$$

If we define an average dislocation by

$$D_0 = \frac{1}{L} \int_{-\infty}^{\infty} D_0(\xi)\, d\xi \quad (28)$$

we have

$$\frac{\sqrt{4k_T k_L \psi_0}}{k_T k_L} = w D_0 L \quad (29)$$

Inserting this into (25), we get

$$|A(\omega)| = \frac{w D_0 L}{\left\{1 + \left(\frac{\cos\theta}{c} - \frac{1}{v}\right)^2 \left(\frac{\omega}{k_L}\right)^2\right\}^{1/2} \{1 + (\omega/k_T)^2\}^{1/2}} \quad (30)$$

for our first model. Since the above function decreases proportionally to ω^{-2} for large ω, we shall call this the 'ω-square model.'

On the other hand, the source factor of amplitude spectral density for our second model will decrease proportionally to ω^{-3} for large ω. Φ_0 is equal to $L^2 D_0^2 k_L k_T^3/8$, according to *Haskell*. Inserting this into (24) and (28), we obtain:

$$|A(\omega)| = \frac{w D_0 L}{\left\{1 + \left(\frac{\cos\theta}{c} - \frac{1}{v}\right)^2 \left(\frac{\omega}{k_L}\right)^2\right\}^{1/2} \left\{1 + \left(\frac{\omega}{k_T}\right)^2\right\}} \quad (31)$$

We shall call this the 'ω-cube model.'

Assumption of Similarity

The straightforward way of testing the earthquake source models proposed above is to compare the predicted spectrum directly with the observed one. For this purpose, however, we must know about such effects of the propagation medium as dissipation and complex interferences on the seismic spectrum for a wide frequency range. Although such knowledge has been accumulating, especially for long-period waves [cf. *Press*, 1964], it does not yet satisfactorily cover the frequency range required for the present study.

As mentioned in the preceding section, we will remove this difficulty by comparing seismic waves having a common propagational path but coming from earthquakes of different sizes. Further, in order to specify an earthquake by a single source parameter, 'magnitude,' we must reduce to one the number of parameters appearing in (30) and (31) by assuming that they are related to each other in some manner.

The simplest of such assumptions may be that large and small earthquakes are similar phenomena. If any two earthquakes are geometrically similar, the fault width w is proportional to the length L. If they are physically similar, all the nondimensional products formed by the source parameters will be the same. The average dislocation D_0 will be proportional to L and, consequently, to w. This implies that if an earthquake is a Starr fracture, the pre-existing stress or strength is constant and independent of source size [*Tsuboi*, 1956]. Since the wave velocity is practically independent of source and may be considered constant for our present purpose, all the quantities having the dimension of velocity must also be constant and independent of source size. Thus, the similarity assumptions imply that the rupture velocity v is a constant and that all the quantities having the dimension of time, such as k_T^{-1} and $(vk_L)^{-1}$, are proportional to L.

For simplicity, we shall further assume that $\cos\theta = 0$ and that $vk_L = k_T$. A value of k_T greater than vk_L may be a more realistic choice, because k_T^{-1} is related to the time required for formation of fracture across the fault width, whereas $(vk_L)^{-1}$ is related to the time required for propagation of fracture along the length of the fault. We shall examine later the case in which $10\ vk_L = k_T$. Essentially the same result as when $vk_L = k_T$ will be obtained, except for the value of k_T corresponding to a source size.

Scaling Law of Seismic Spectrum

Under the assumptions described in the preceding section, we can express the source factor of amplitude spectral density as a function of L, ω, and several nondimensional constants. Taking L as a parameter, we shall obtain a group of curves of spectral density, each of which corresponds to an earthquake of a certain size. In order to find which curve corresponds to a given earthquake size, we must have a scale to measure size. The most convenient scale for our purpose is the surface wave magnitude scale, defined by *Gutenberg and Richter* [1936]. This magnitude, designated as M_s, is proportional to the logarithm of amplitude of teleseismic surface waves with period of about 20 sec. Since at this period the waves are usually well dispersed, we may express the wave train $y(t)$ by the stationary phase approximation, as follows:

$$y(t) = \frac{1}{\pi}\int_{-\infty}^{\infty} |Y(\omega)| \cos(\omega t + \delta(\omega))\, d\omega \approx \frac{|Y(\omega_0)|}{\sqrt{2\pi\,|d^2\delta/d\omega^2|_{\omega=\omega_0}}} \cdot \cos\left(\omega_0 t + \delta(\omega_0) \pm \frac{\pi}{4}\right) \tag{32}$$

where ω_0 is given by the equation

$$t = -(d\delta/d\omega)_{\omega=\omega_0} \tag{33}$$

If this approximation is valid, the trace amplitude of waves with frequency ω_0 read directly on the record will be proportional to the spectral density $|Y(\omega_0)|$. The quantity $d^2\varphi/d\omega^2$ in (32) is the sum of a propagation term and a source term. Since the propagation term is proportional to the travel distance, the source term may be neglected at long distances. Thus, we may assume that the trace amplitude of surface waves with period of 20 sec is equal to the amplitude spectral density of waves with that period, except for a factor that is independent of the source size. The validity of this assumption is confirmed by comparing the ratio of trace amplitudes of Love waves with a certain period from two aftershocks of the Kern County earthquake with the ratio of amplitude spectral densities at that period obtained by the Fourier analysis method. Both ratios agree well.

Thus, the dependence of amplitude spectral density, $|A(\omega)|$, on the magnitude M_s will be such that $\log|A(\omega)|$ at the period of 20 sec is equal to M_s plus a constant. In other words, two spectrum curves corresponding to two earthquake sizes differing by $M_s = 1.0$ will be separated by 1.0 along the ordinate at the period of 20 sec, if the curve $|A(\omega)|$ is drawn on a logarithmic scale. Figures 3 and 4 shows such groups of curves for the ω-square and ω-cube models, respectively.

The curves shown in each of these charts have an identical shape. The frequency that characterizes the shape of the curve, such as k_T, is proportional to L^{-1}, and the spectral density at $\omega = k_T$ is proportional to L^3, as can be found from (30) and (31) under the assumption of similarity. Therefore, the points corresponding to the characteristic frequency lie on a straight line with gradient 3, as shown by dashed lines in Figures 3 and 4. As mentioned

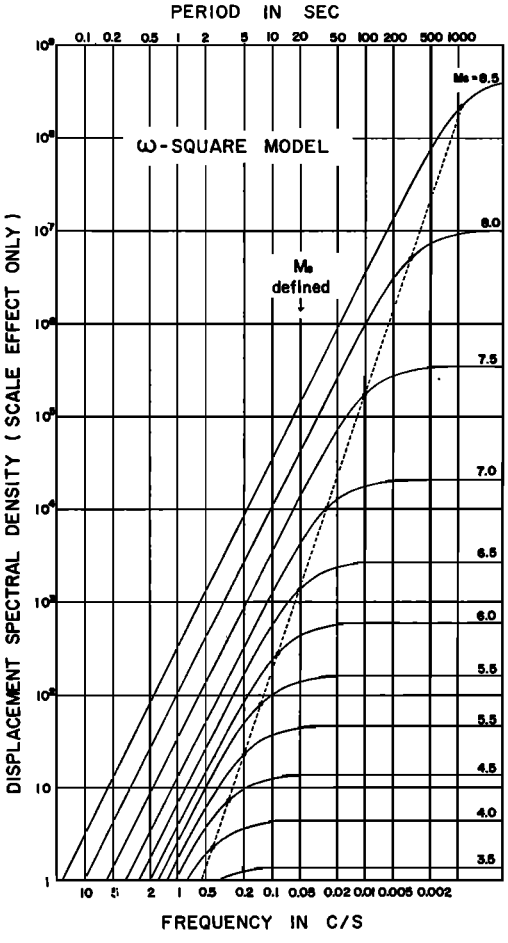

Fig. 3. Dependence of amplitude spectral density of earthquake magnitude M_s for the ω-square model.

before, the spacing of curves for different earthquake magnitudes is determined by the definition of M_s. The definition alone, however, cannot give the absolute value of magnitude corresponding to each curve.

If we know the absolute value for one of the curves, the values for the rest are determined from the definition of M_s. First we adopt a trial value of magnitude for one of the curves and assign magnitude values to other curves according to the definition. Then we can find the ratio of spectral densities for two different magnitudes as a function of frequency or period. This ratio is compared with the observed one given by *Berckhemer* [1962]. His data include six sets of two earthquakes with the same epicenter but of different magnitudes. The magnitude of earthquakes studied by him covers the range 4.5 to 8. After several trials, we choose the absolute value of magnitude that gives the best agreement between theory and observation. The values assigned to the curves in Figures 3 and 4 are determined in this manner, and the corresponding theoretical spectral ratios are shown in Figure 5, together with the observed ratios given by Berckhemer.

Love Waves from Two California Shocks

The applicability of the theoretical curves of spectral densities obtained in the preceding section is tested by the use of records of Love waves from two aftershocks of the Kern County, California, earthquake of 1952. The epicenters of these two earthquakes are within several miles of each other, according to *Richter* [1955], and they show identical first motion patterns, according to *Båth and Richter*

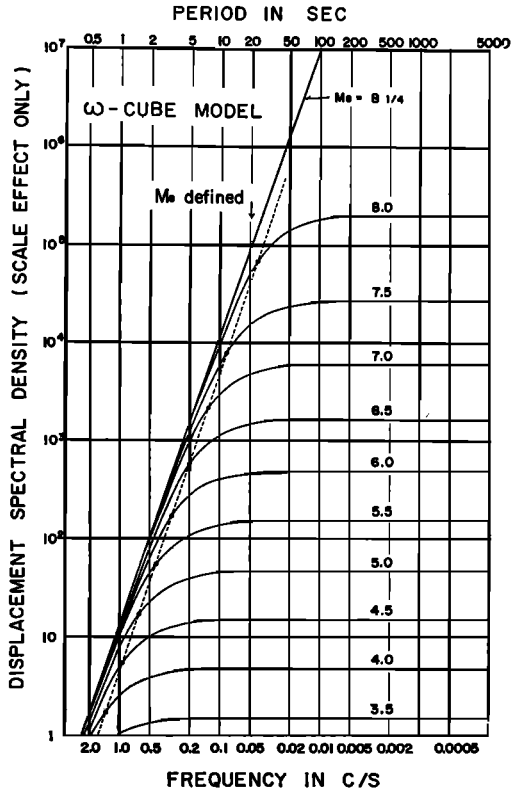

Fig. 4. Dependence of amplitude spectral density on earthquake magnitude M_s for the ω-cube model.

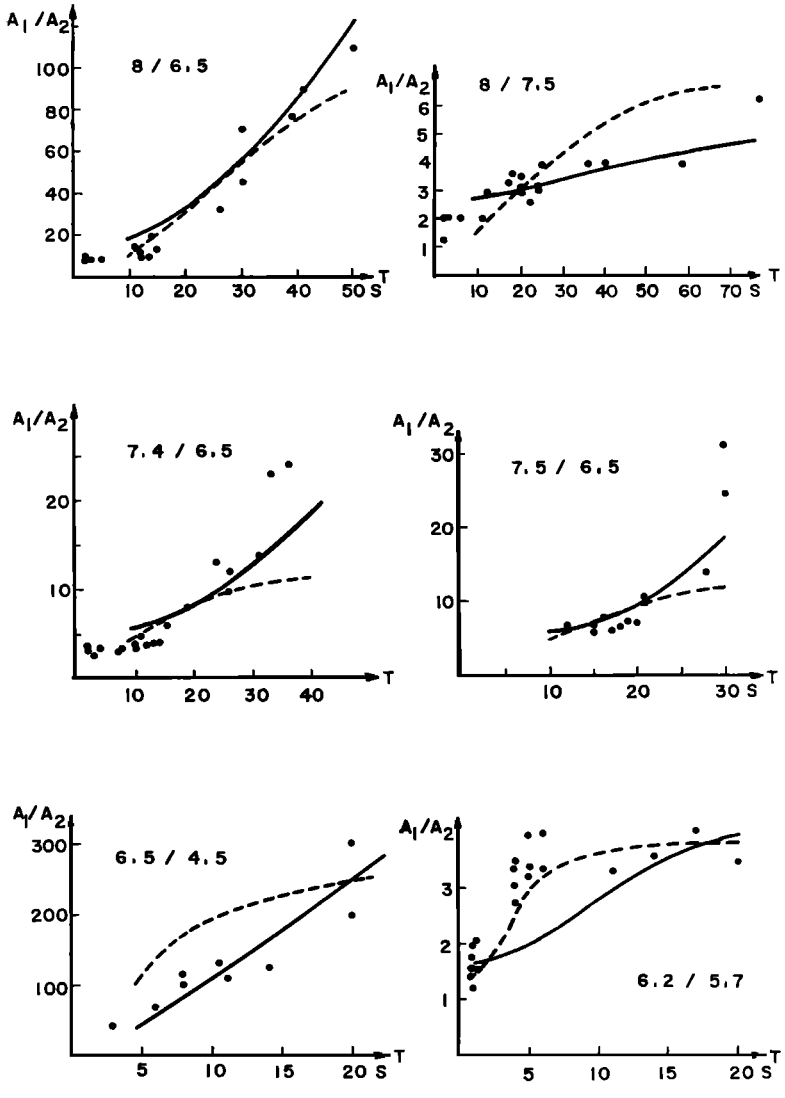

Fig. 5. Comparison of theoretical and observed spectral ratio, plotted against period, for pairs of earthquakes having nearly the same epicenter but different size. Observed values are reproduced from *Berckhemer* [1962]. The numbers shown for each pair are the earthquake magnitude for the pair. Solid line denotes ω-square model; dashed line denotes ω-cube model.

[1958]. The Richter magnitude (M_L; local scale for southern California) of one of them is 6.1, and that of the other is 5.8. The difference of 0.3 corresponds to the maximum amplitude ratio of 2 on the record of the standard Wood-Anderson seismograph.

The amplitude ratios of Love waves from the two earthquakes observed at Weston, Ottawa, and Resolute Bay are shown in Figure 6. They are obtained by Berckhemer's method, in which the ratio is obtained between the corresponding peaks of waves by directly reading amplitudes on the record. As shown in Figure 7, the correspondence of peaks and troughs between the two earthquakes is excellent, and there is no difficulty in obtaining such ratios. Figure 8 shows the ratio of the amplitude spectral density obtained by the Fourier analysis method.

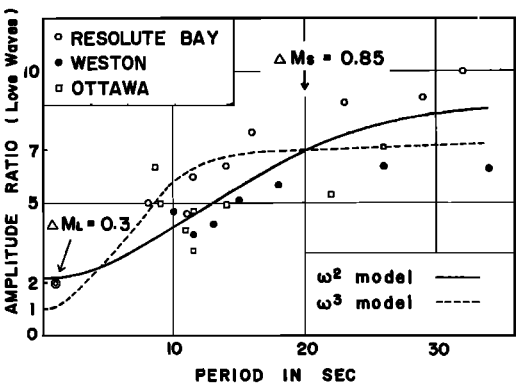

Fig. 6. Comparison of theoretical and observed spectral ratio for two aftershocks of the Kern County, California, earthquake of 1952. Observed ratios are obtained from trace amplitude.

There is no significant difference between the results obtained by the two methods, justifying the simple procedure used by Berckhemer.

The theoretical curves of spectral density ratio for an earthquake pair with magnitudes M_s around 6.0 which best fit the observations are shown in these figures. It is remarkable that the observed ratio is about 7 at the period of 20 sec; in other words, the difference in M_s between the two earthquakes is 0.85, about 3 times larger than the difference in M_L obtained by Richter. Our ω-square model explains this fact satisfactorily, because M_L must have been measured on waves with periods of less than 1 sec, and this model predicts a spectral density ratio of about 2 at these periods. On the other hand, the ω-cube model predicts nearly the same spectral density at short periods for the two earthquakes and does not explain the observation.

A more general comparison of the local magnitude scale M_L and the surface wave magnitude scale M_s is difficult. The maximum amplitude recorded by the Wood-Anderson seismograph would not be directly proportional to the amplitude spectral density at any fixed period, because the signal duration and prevailing period may change with the earthquake source size. The spectral ratio may be nearly equal to the maximum amplitude ratio for such earthquakes with small difference in magnitude as studied in the present section, but the equality cannot hold for larger magnitude difference. Further, the empirical relation between M_L and M_s, with which the theoretical relation is to be compared, has not yet been stabilized [*Richter*, 1958].

Relation Between m_B and M_s

On the other hand, the relation between the magnitude scale m_B, defined as the logarithm of amplitude of teleseismic body waves, and M_s has been well established empirically by *Gutenberg and Richter* [1965*a*]. Further, it is well known that the usual record of teleseismic body waves, obtained by a standard short-period seismograph such as Benioff's, shows a rather narrow spectral band around 1 c/s. Therefore, we may correlate the amplitude of body waves with the spectral density at 1 c/s.

If our signal is a finite portion of a Gaussian

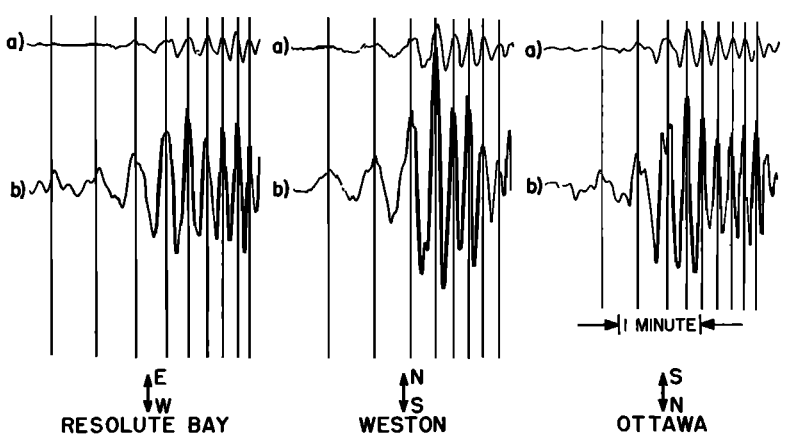

Fig. 7. Love waves from the Kern County aftershocks (no. 194 above, no. 141 below; numbers assigned by *Richter* [1955]) recorded at Ottawa, Resolute, and Weston.

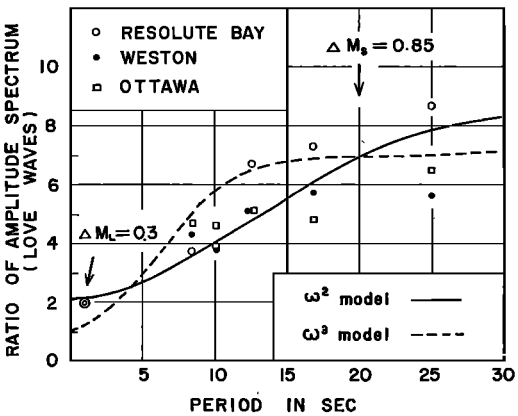

Fig. 8. Comparison of theoretical and observed spectral ratio for two aftershocks of the Kern County, California, earthquake of 1952. Observed spectral ratios are obtained by Fourier analysis.

noise, the amplitude spectral density will be proportional to the square root of the signal duration. On the other hand, if the signal is a finite portion of a coherent sinusoidal oscillation, the spectral density will be proportional to the signal duration. We may assume that the actual seismic signal has an intermediate nature between the above two extremes. Then, we may write the spectral density at 1 c/s as follows:

$$A(1) = \text{const} \times A_m \times t^{0.5 \sim 1.0} \qquad (34)$$

where A_m is the maximum trace amplitude and t is the signal duration.

According to *Gutenberg and Richter* [1956*b*], $\log t$ is related to m_B by the empirical formula

$$\log t = -1.9 + 0.4 m_B \qquad (35)$$

Inserting this equation into (34), we obtain

$$\log A(1) = \text{const} + (1.2 \sim 1.4) m_B \qquad (36)$$

From this equation and the charts of spectral density curves given in Figures 3 and 4, we can obtain the theoretical relation between m_B and M_s on the basis of the ω-square and ω-cube models. The constant in (36) is determined in such a way that m_B and M_s agree at 6.75, in accordance with the Gutenberg-Richter empirical formula

$$m_B = 6.75 + 0.63(M_s - 6.75) \qquad (37)$$

Figure 9 shows the relation between m_B and M_s for the ω-square and ω-cube model. The shaded area indicates the range between the above-mentioned two extreme cases of the dependence of spectral density on signal duration. The theoretical curve for the ω-cube model does not agree with the empirical one given by Gutenberg and Richter. On the other hand, the agreement is excellent for the ω-square model, except for smaller magnitudes. Looking at the original data from which Gutenberg and Richter derived their empirical formula, we find that the theoretical curve based on the ω-square model better explains the observations at small magnitudes than the empirical curve as shown in Figure 10. This result strongly supports the applicability of the scale law of seismic spectrum derived from the ω-square model on the assumption of similarity.

Relation Between Fault Length and M_s for the ω-Square Model

In deriving the scaling law of seismic spectrum we assumed that the characteristic frequency k_T is proportional to L^{-1}. We can check this assumption against geological or geodetic observations on an earthquake fault of known magnitude M_s. The value of k_T for a given M_s is found from the theoretical curves for the ω-square model shown in Figure 3. Then k_T^{-1} should be proportional to L, if the assumption of similarity holds. Figure 11 shows the rela-

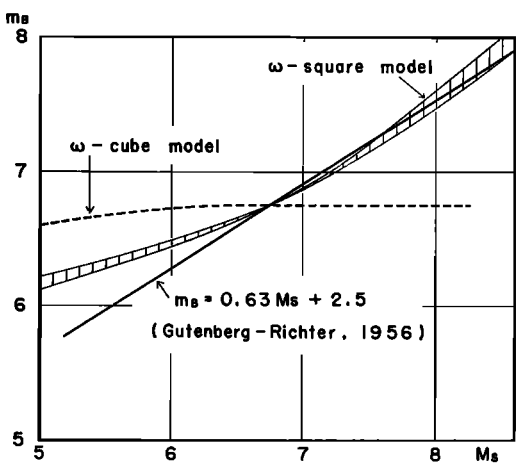

Fig. 9. Theoretical relation between m_B and M_s based upon the ω-square and ω-cube models, as compared with the Gutenberg-Richter empirical formula.

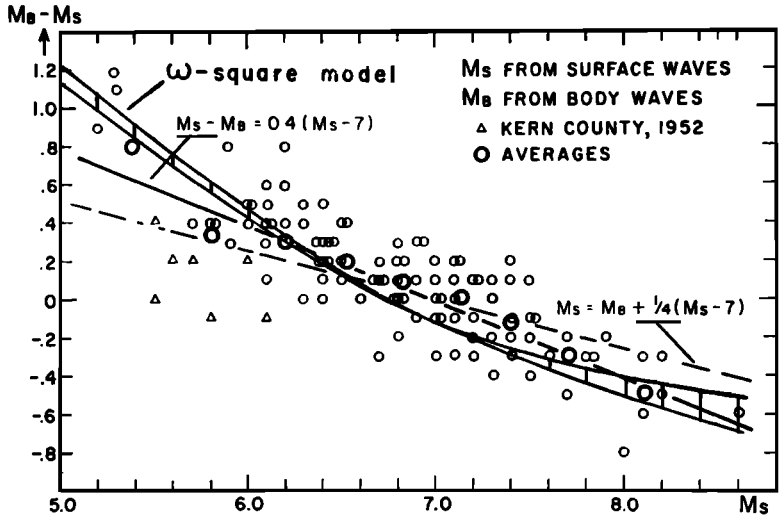

Fig. 10. Theoretical relation between m_B and M_s based upon the ω-square model, as compared with that observed by *Gutenberg and Richter* [1965a].

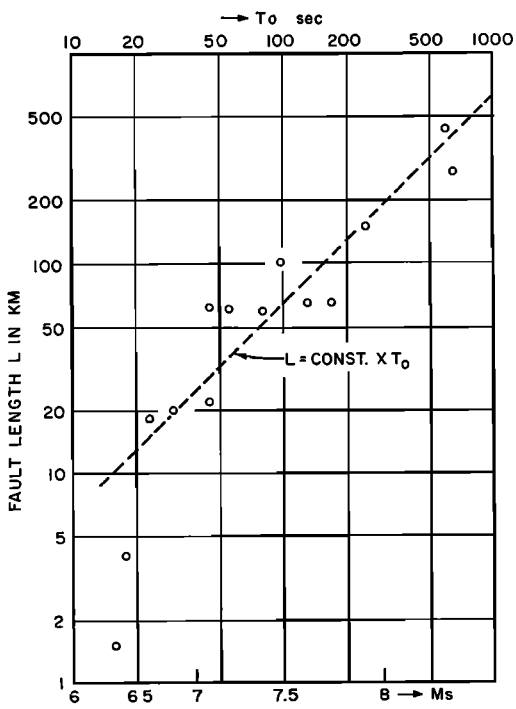

Fig. 11. Relation between the length of earthquake fault measured by geological or geodetic means and the characteristic time of the earthquake determined from its magnitude on the basis of the ω-square model. A linear relation between them supports the assumption of similarity.

tion between $T_0 = 2\pi k_T^{-1}$ and L for the earthquake fault given in Tocher's list [*Tocher*, 1960]. A linear relationship holds between L and T_0, if earthquakes smaller than magnitude 6.5 are excluded. In the case of small earthquakes, the surface evidence may not reveal the true fault length at the earthquake focus. There is also such an ambiguity with the magnitude of small earthquakes that the magnitude given in Tocher's list may or may not be taken as M_s. Considering these facts, we may conclude from Figure 11 that geological data do not exclude the assumption of similarity.

The characteristic time T_0 for a given M_s as shown in Figure 11 may seem a little too large. It is possible to reduce this value without affecting significantly the conclusions obtained above. If we assume that $k_T = 10\ vk_L$ instead of $k_T = vk_L$, and if we determine a set of spectral density curves using the data of Berckhemer and others as given above, we find that the value of T_0 becomes about one-third that given in Figure 11. The agreement between theory and observation is as good as that shown in Figures 5, 6, and 8, and we find again that the ω-square model explains the relation between m_B and M_s and that the ω-cube model does not.

Efficiency of Seismic Radiation

Let us now examine the efficiency of seismic

energy radiation, which must be independent of earthquake source size if the similarity condition holds strictly. We define the efficiency as the ratio of the energy radiated in the form of seismic waves to the elastic energy released by the formation of an earthquake fault. If an earthquake is a Starr fracture [*Starr*, 1928], the fault-released elastic energy is proportional to D_0^2L. Under the assumption of similarity, this energy will be proportional to L^3. If we know the energy for a certain value of M_s, we can determine the value for any M_s from the scaling law given in the preceding section. Assuming that $\log E$ is 23.7 for $M_s = 7.5$ from the result of the writer's study on the Niigata earthquake [*Aki*, 1966], we get the released strain energy for various M_s as shown in Table 1. The energy radiated in the form of seismic waves is evaluated by the Gutenberg-Richter formula

$$\log E = 11.4 + 1.5M_s \qquad (38)$$

and is also shown in Table 1 together with its ratio to the strain energy. The ratio definitely increases with decreasing magnitude. Thus, starting with the assumption of similarity, we have ended by denying it.

It is, however, not impossible that a further refinement of the magnitude-energy relation (38) may eventually support the assumption of similarity with regard to the radiation efficiency, because (38) is based upon several simplified assumptions.

It should be noted here that *Båth and Duda* [1964], using Berckhemer's result [*Berckhemer*, 1962], reached an entirely different conclusion on the radiation efficiency. They found that the efficiency increases with increasing magnitude of the earthquake. This difference may be attributed to a difference in the assumed source model. As mentioned before, the model of Berckhemer, if interpreted by dislocation theory, is the one in which the dislocation is constant and independent of source size, but the dislocation in our model is proportional to the linear dimension of the source.

TABLE 1. Released Strain Energy, Seismic Wave Energy and Efficiency of Seismic Radiation

M_s	$\log E_{st}$	$\log E_w$*	E_w/E_{st}
8.5	26.7	24.2	0.003
8.0	25.2	23.4	0.016
7.5	23.7	22.7	0.10
7.0	22.5	21.9	0.25
6.5	21.6	21.2	0.40

* $\log E_w = 11.4 + 1.5\,M_s$.

Departure from Similarity

As mentioned before, the assumption of similarity implies a constant stress drop in all earthquakes. If the stress drop differs for two earthquakes, our scaling law will not apply. If the stress drop varies systematically with respect to such environmental factors as focal depth, orientation of fault plane, and crust-mantle structure, we may construct different scaling laws for different environments. Such a study of the seismic spectrum may eventually reveal the distribution of stress drop or strength of material in the earth's crust and mantle. For such a study, however, we shall need more precise measurements of spectrum over wider ranges of frequency than are now available, as well as detailed knowledge of the propagation factor of the spectrum.

Even with the present limited knowledge of the propagation factor, however, we may demonstrate remarkable differences in stress drops between some earthquakes by the use of long-period surface waves. The earthquakes to be compared here are the Niigata earthquake of June 16, 1964, and the Parkfield (California) earthquake of June 28, 1966.

The stress drop in the Niigata earthquake was obtained by the following procedure [*Aki*, 1966]. The geometry of fault movement was determined from the radiation patterns of P waves, S waves [*Hirasawa*, 1966], and G waves. The spectral density of displacement due to G waves was estimated for periods of 50 to 200 sec, corrected for dissipation and geometric spreading, and compared with the theoretical excitation function [*Haskell*, 1964; *Ben-Menahem and Harkrider*, 1964] corresponding to a source of that geometry. From this comparison we estimated the product of rigidity μ, area S of fault surface, and average dislocation Δu, which corresponds to the moment M_0 of the component couple of the equivalent doublet [*Maruyama*, 1963; *Burridge and Knopoff*, 1964; *Haskell*, 1964]. The value of M_0 ($= \mu\,\Delta u S$)

for the Niigata earthquake was 3×10^{27} dynes cm. All the near field evidence (echo-sounding survey, aftershock epicenters, and Tsunami source area) indicated a fault length, L, of about 100 km. The focal depths of the main shock and aftershocks indicated a fault width, w, of about 20 km. Assuming that $\mu = 3.7 \times 10^{11}$ dynes cm^{-2}, corresponding to a shear velocity of 3.6 km/sec and density of 2.85 g/cm^3, we obtained the value of the average dislocation as 400 cm by inserting the values of L, w, and μ into the equation $M_0 = \mu \, \Delta u \cdot Lw$. This value agrees well with those observed by echo-sounding surveys made just before and after the earthquake [*Mogi et al.*, 1965]. Finally, the stress drop was estimated as about 125 bars with the aid of Starr's theory [*Starr*, 1928].

Now, let us compare the Niigata earthquake with the Parkfield earthquake. The Parkfield earthquake took place right on the San Andreas fault near Cholame and Parkfield. The PDE card of the Coast and Geodetic Survey reports the epicenter as (35.9°N, 120.5°W), and the origin time as 04:26:12.4 GCT, June 28, 1966. The magnitude is 5.8, 5.5, and 6½ as given by the Pasadena, Berkeley, and Palisades stations, respectively. According to a personal communication from Clarence R. Allen and Stewart W. Smith of the California Institute of Technology, the near field measurements revealed a strike slip fault associated with this earthquake, its length being about 38 km and its offset about 5 cm.

$G2$ waves from this earthquake are clearly recorded by long-period seismographs at Resolute ($\Delta = 40°$) and at Ottawa ($\Delta = 35°$). The peak-to-peak amplitudes on the records at a period of 70 sec are a little over 1 mm at both stations. This corresponds to a spectral density of ground displacement of about 0.04 cm sec at that period.

The $G2$ waves from the Niigata earthquake at the epicentral distance of 35° to 40° show a spectral density of about 1.6 cm sec at a period of 70 sec for a certain radiation azimuth. If the Niigata earthquake source is a strike slip fault like the Parkfield earthquake, and if we observed G waves in the direction of maximum radiation, we would expect a spectral density of about 5 cm sec at a period of 70 sec for $G2$ waves at $\Delta = 35° \sim 40°$. This value is about 125 times as large as that observed from the Parkfield earthquake. Considering that the effect of finite size was significant for the Niigata earthquake (about a factor of ½ at a period of 70 sec) but probably not for the Parkfield earthquake, we estimate the ratio of the source moment M_0 for the Parkfield earthquake to that for the Niigata earthquake as 1/250. Thus, we get a moment value of about 1×10^{25} dynes for the Parkfield earthquake.

Using the same rigidity value as for the Niigata earthquake and the observed values of fault length and dislocation mentioned before, we get a fault width of about 13 km from the above value of moment. This value of fault width gives us an extremely low estimate of strain release. Since Knopoff's fracture model is more appropriate for a strike slip than Starr's, we estimate the strain release by the formula $\epsilon = \Delta u/2w$ [*Knopoff*, 1958]. We get a value of ϵ of 2×10^{-6} and a corresponding stress drop of about 0.7 bar, which is indeed a remarkably low value. Even if there is an order of magnitude error in estimating the value of moment, the stress drop is still several bars.

As mentioned before, if the stress drop is different between two earthquakes, the scaling law derived in the present paper will not apply to them. We found some indication of violation of the scaling law when we compared the Parkfield earthquake with one of the aftershocks of the Kern County earthquake.

The magnitude of the Parkfield earthquake given by local stations is 5.5 (Berkeley) ~ 5.8 (Pasadena). The surface wave magnitude M_s of this earthquake, calculated from the Love wave amplitude at a period of 20 sec recorded at Ottawa, is 6½. This value agrees with the magnitude given by the Palisades station.

On the other hand, the magnitude of number 141 aftershock [*Richter*, 1955] of the Kern County earthquake is 6.1. M_s for this earthquake, calculated also from Love wave amplitude at a period of 20 sec recorded at Ottawa, is 6.2.

Since the variability of seismic amplitudes is very large, it is dangerous to draw any conclusions from measurements at a few stations. However, the magnitude values above suggest that the spectral density for the Parkfield earthquake may be greater than that for the Kern County aftershock at long periods, and smaller at short periods. If so, the two spec-

trum curves must cross each other, violating the scaling law. This result is expected if the stress drop in the Parkfield earthquake is lower than that in the Kern County aftershock. The reduction of stress drop is equivalent to the reduction of D_0 in (30), and it will shift the spectrum curves in Figure 3 downward parallel to the ordinate, causing an intersection with the original curve in the manner described above.

As we have seen above, there is a possibility that the stress drop in an earthquake may vary greatly according to its geological environment. We shall probably have to assign different scaling laws to different environments. This implies that a single parameter, such as magnitude, cannot describe an earthquake even as a rough measure. The measurement of seismic spectral density rather than amplitude will become increasingly important. To understand the observed spectrum in terms of the physics of the earthquake source, however, we shall have to know more about the effect of the propagation media on the spectrum than we do now.

Acknowledgments. I should like to thank Dr. J. H. Hodgson for making the Ottawa and Resolute records of the Parkfield earthquake available to me.

This research was supported by the Advanced Research Projects Agency and was monitored by the Air Force Office of Scientific Research under contract AF49(638)-1632.

References

Aki, K., Correlogram analysis of seismograms by means of a simple automatic computer, *J. Phys. Earth, 4,* 71–79, 1956.

Aki, K., Generation and propagation of *G* waves from the Niigata earthquake of June 16, 1964, 2, Estimation of earthquake moment, released energy, and stress-strain drop from the *G* wave spectrum, *Bull. Earthquake Res. Inst. Tokyo Univ., 44,* 73–88, 1966.

Asada, T., On the relation between the predominant period and maximum amplitude of earthquake motions, *J. Seismol. Soc. Japan, Ser. 2, 6,* 69–73, 1953.

Båth, M., and S. J. Duda, Earthquake volume, fault plane area, seismic energy, strain, deformation, and related quantities, *Ann. Geofis. Rome, 17,* 353–368, 1964.

Båth, M., and C. F. Richter, Mechanism of the aftershocks of the Kern County, California, earthquake of 1952, *Bull. Seismol. Soc. Am., 48,* 133–146, 1958.

Ben-Menaham, A., and D. G. Harkrider, Radiation patterns of seismic surface waves from buried dipolar point sources in a flat statified earth, *J. Geophys. Res., 69,* 2605–2620, 1964.

Berckhemer, H., Die Ausdehnung der Bruchfläche im Erdbebenherd und ihr Einfluss auf das seismische Wellenspektrum, *Gerlands Beitr. Geophys., 71,* 5–26, 1962.

Burridge, R., and L. Knopoff, Body force equivalents for seismic dislocations, *Bull. Seismol. Soc. Am., 54,* 1875–1888, 1964.

Byerly, P., The periods of local earthquake waves in central California, *Bull. Seismol. Soc. Am., 37,* 291–298, 1947.

Gutenberg, B., and C. F. Richter, On seismic waves, *Gerlands Beitr. Geophys., 47,* 73–131, 1936.

Gutenberg, B., and C. F. Richter, Earthquake magnitude, intensity, energy, and acceleration, *Bull. Seismol. Soc. Am., 32,* 163–191, 1942.

Gutenberg, B., and C. F. Richter, Earthquake magnitude, intensity, energy, and acceleration, 2, *Bull Seismol. Soc. Am., 46,* 105–145, 1956*a*.

Gutenberg, B., and C. F. Richter, Magnitude and energy of earthquakes, *Ann. Geofis. Rome, 9,* 1–15, 1956*b*.

Haskell, N., Total energy and energy spectral density of elastic wave radiation from propagating faults, *Bull. Seismol. Soc. Am., 54,* 1811–1842, 1964.

Haskell, N., Total energy and energy spectral density of elastic wave radiation from propagating faults, 2, A statistical source model, *Bull. Seismol. Soc. Am., 56,* 125–140, 1966.

Hirasawa, T., Source mechanism of the Niigata earthquake of June 16, 1964, as derived from analysis of body waves, *J. Phys. Earth, 14,* in press, 1966.

Honda, H., and H. Ito, On the period of the *P* waves and the magnitude of the earthquake, *Geophys. Mag., 13,* 155–160, 1939.

Jones, A. E., Empirical studies of some of the seismic phenomena of Hawaii, *Bull. Seismol. Soc. Am., 28,* 313–338, 1938.

Kanai, K., K. Osada, and S. Yoshizawa, The relation between the amplitude and the period of earthquake motion, *Bull. Earthquake Res. Inst. Tokyo Univ., 31,* 45–56, 1953.

Kashara, K., The nature of seismic origin as inferred from seismological and geodetic observations, 1, *Bull. Earthquake Res. Inst. Tokyo, 35,* 747–532, 1957.

Knopoff, L., Energy release in earthquakes, *Geophys. J., 1,* 44–52, 1958.

Maruyama, T., On the force equivalents of dynamic elastic dislocations with reference to the earthquake mechanism, *Bull. Earthquake Res. Inst. Tokyo Univ., 41,* 467–486, 1963.

Matumoto, T., On the spectral structure of earthquake waves, *Bull. Earthquake Res. Inst. Tokyo, 38,* 13–28, 1960.

Matuzawa, T., Study of earthquakes, *Ūno Shoten,* Tokyo, pp. 45, 207, 1964.

Mogi, A., B. Kawamura, and Y. Iwabuchi, Submarine crustal movement due to the Niigata earthquake in 1964, in the environs of the Awa

Shima Island, Japan Sea, *J. Geodetic. Soc. Japan, 10,* 180–186, 1965.

Press, F., Long period waves and free oscillations of the earth, in *Research in Geophysics,* vol. 2, chapter 1, pp. 1–26, The M.I.T. Press, Cambridge, Mass., 1964.

Richter, C. F., Foreshocks and aftershocks, Earthquakes in Kern County, California, during 1952, *Calif Dept. Nat. Resources, Div. Mines, Bull. 171,* 177–198, 1955.

Richter, C. F., *Elementary Seismology,* p. 347, W. H. Freeman and Co., San Francisco, 1958.

Starr, A. T., Slip in a crystal and rupture in a solid due to shear, *Proc Cambridge Phil. Soc., 24,* 489–500, 1928.

Tocher, D., Movement on faults, *Proc. 2nd World Conf. Earthquake Engineering, 1,* 551–564, 1960.

Tsuboi, C., Earthquake energy, earthquake volume, aftershock area, and strength of the earth's crust, *J. Phys. Earth, 4,* 63–66, 1956.

(Received September 17, 1966.)